2023 IEEE Wireless Communications and Networking Conference (WCNC) | 978-1-6654-9122-8/23/$31.00 ©2023 IEEE | DOI: 10.1109/WCNC55385.2023.10118600

An Effective Deployment Scheme for Elimination of Phase Cancellation in Backscatter-based WPCN

Qiang Wang*, Yuzhuo Ma*, Chenglong Zhang*, Tang Liu*†, Jilin Yang*†, Dié Wu*†
*College of Computer Science, Sichuan Normal University, Chengdu, Sichuan, China
†Visual computing and virtual reality Key Lab, Sichuan Normal University, Chengdu, Sichuan, China

***Abstract*—Without the need for batteries, backscatter-based Wireless Powered Communication Network (WPCN) has been envisioned as a promising alternative to conventional wireless networks. Unfortunately, the unique phase cancellation problem in backscatter-based WPCN is essentially a phenomenon that severely affects connectivity and reliability of the network. Many arts have tried to tackle this issue either by using multiple antennas to employ the signal diversity, which increases the size and is not cost-efficient, or by making a repetition of the same information with different load impedances, which significantly decreases the throughput of network. In our paper, we propose an effective deployment scheme, aiming to fundamentally eliminate the phase cancellation problem. Specifically, we first build a practical communication model seeking the blind areas caused by phase cancellation. Then, a greedy algorithm and a minimum-weight graph based algorithm are proposed to elaborate topology of the network to ensure the connectivity. Finally, extensive experiments are carried out to evaluate the performance.**

***Index Terms*—Backscatter communication, phase cancellation, deployment, WPCN.**

I. Introduction

The rapid development of Internet of Things (IoT) has spurred research into providing ubiquitous connectivity for everyone and everything. However, the limited battery capacity is turned out to be the main bottleneck that stunts the widespread adoption of traditional IoT devices. Fortunately, by harvesting energy from ambient radio frequencies (e.g., WiFi [1], cellular [2], Bluetooth [3] and FM radios [4-5]), backscatter communication has emerged as a new paradigm that enables IoT devices to work permanently without the need for batteries. Consequently, backscatter-based Wireless Powered Communication Network (WPCN) [6] that consists of passive nodes employing backscatter technology is now envisioned as a promising alternative to conventional wireless networks in the near future [7-8].

Despite backscatter-based WPCN is one such network that opens up many possibilities in the world of IoT, there still exists a gap between the potential and reality. Unlike active nodes, the backscatter-based passive nodes are radio-less, and they can not afford the cost introduced by traditional signal processing components. Instead, a low-power backscatter modulator and a simple envelope detector are employed for communication, which result in the inevitable occurrence of the phase cancellation problem [9]. For better illustration, Fig. 1(a) depicts a typical communication scenario. When

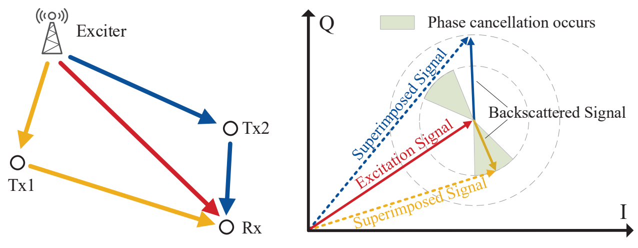

(a) Communication scenario (b) Phase cancellation phenomenon

Fig. 1. Illustration for phase cancellation.

transmitting, the transmitter (Tx1 or Tx2) modulates its information by reflecting or absorbing the excitation signal broadcasted by the exciter (e.g., TV tower or dedicated source). At the receiver (Rx), the backscattered signal is superimposed with the excitation signal, and the resultant signal (blue or yellow dotted vector in Fig. 1(b)) is demodulated by the envelope detector. Unfortunately, since the simple envelope detector is only able to detect the amplitude information but not the phase, once the amplitude difference between the superimposed signal and the excitation signal is imperceptible (refer to the yellow dotted and red solid vectors), the information contained in the resultant signal would be completely cancelled, and the communication would fail. Thus, how to eliminate phase cancellation which is a ubiquitous problem in all backscatter-based WPCNs so as to ensure the connectivity and reliability has become a critical issue.

To alleviate the severe impacts introduced by phase cancellation, one possible way is to utilize multihop network to flood the information to enhance the transmission reliability [10-11]. Nevertheless, due to the ubiquitous occurrence of phase cancellation, every passive node is possible of dropping into the blind area where the information is completely cancelled. That is to say, if the network's topology is not carefully elaborated in prior, there might not exist a feasible route from the transmitter to the destination at all. Therefore, an urgent requirement is to investigate how phase cancellation affects the performance of the network, and use it as a guidance for the deployment of a reliable backscatter-based WPCN.

In this article, we propose an effective deployment scheme, aiming to eliminate phase cancellation problem in backscatter-based WPCN. Specifically, we first build a practical communication model with phase cancellation, and seek for signal blind areas. Then, to ensure the connectivity of the network, a group of passive nodes acting as sinks and relays is deployed outside of the blind area, where sinks are introduced to collect and forward information while relays are used to form a

This work is partially supported by the National Natural Science Foundation of China (62002250, 62072320), the Natural Science Foundation of Sichuan Province (2022NSFSC0569, 2022NSFSC0929).
Corresponding author: Dié Wu (Email: wd@sicnu.edu.cn).

978-1-6654-9122-8/23/$31.00 ©2023 IEEE

connected network. Thus, our objective can be divided into two folds: (i) how to utilize as few sinks as possible to provide all passive nodes in the field with data transmission service. (ii) how to construct a connected network with as few relays as possible. Generally, we are facing the following challenges. The first challenge is to explore the relationship between the nodes' locations and their communication reliability. The second challenge is to select the appropriate locations for sinks and relays from a continuous space.

The contributions of our work are summarized as follows.

- We build a communication model with phase cancellation, which to the best of our knowledge, is the first work that practically reveals how the nodes' locations affect the communication reliability.
- A greedy algorithm and a minimum-weight tree based algorithm are proposed to solve the problem of deploying sinks and relays, which ensures the connectivity of network under the constraint of phase cancellation.
- Extensive experiments are conducted to illustrate the advantages of our scheme. The results show our scheme can turn 300 randomly deployed nodes to be a connected network with only 20 sinks and 9 relays on average.

II. System Model

A. Communication Model

Consider a backscatter-based WPCN wherein the passive nodes employ backscatter modulation, i.e., they transmit their data through altering the reflecting coefficient between absorbing and reflecting states, representing symbol '0' and symbol '1', respectively. For simplicity, we consider the exciter transmits a non-modulated signal of wavelength λ, angular frequency ω, and amplitude A_E, which can be denoted as:

$$v(t) = A_E \cos \omega t. \tag{1}$$

Then, the signals received at transmitter T and receiver R from the exciter E can be expressed respectively as:

$$v_{E\to T}(t) = A_{ET} \cos\left(\omega t + 2\pi \|ET\|/\lambda\right), \tag{2}$$

$$v_{E\to R}(t) = A_{ER} \cos\left(\omega t + 2\pi \|ER\|/\lambda\right), \tag{3}$$

where $\|ET\|$ and $\|ER\|$ represent the distance from E to T and R, respectively. A_{ET} and A_{ER} represent the amplitude of the exciter signal received at T and R, respectively. Hence, the signal reflected from T received at R can be expressed as:

$$v_{T\to R}(t) = A_{TR} \cos\left(\omega t + 2\pi(\|ET\| + \|TR\|)/\lambda + \phi\right), \tag{4}$$

where ϕ is the phase change introduced by reflection, A_{TR} represents the amplitude of reflected signal received at R, and $\|TR\|$ denotes the distance between T and R.

When T is transmitting, R receives the superposition of two signals, i.e., the non-modulated signal from E and the backscattered signal from T. If we let b be either '0' or '1', representing the absorbing and reflecting states, respectively, the superimposed signal received at R can be expressed as:

$$v_R(t) = v_{E\to R}(t) + b \cdot v_{T\to R}(t). \tag{5}$$

Thus, the amplitude of the superimposed signal received at R can be written as:

$$A_R^b(t) = \sqrt{A_{ER}^2 + b\cdot (A_{TR}^2 + 2A_{ER}A_{TR}\cos\beta)}, \tag{6}$$

where $\beta = \phi + 2\pi(\|ET\| + \|TR\| - \|ER\|)/\lambda$ is the backscatter channel phase. As the power is proportional to the square of the amplitude, using Friis propagation formula, the resultant power received at R can be expressed as:

$$P_R^b = \frac{PG_E G_R \lambda^2}{16\pi^2 \|ER\|^2} + \frac{b\gamma^2 PG_E G_T^2 G_R \lambda^4}{256\pi^4 \|ET\|^2 \|TR\|^2} + \frac{b\gamma PG_E \sqrt{G_T^3 G_R}\lambda^3 \cos\beta}{32\pi^3 \|ET\| \|ER\| \|TR\|}, \tag{7}$$

where P represents the output power of E, γ denotes the terminating impedance that determines the strength of the backscattered signal, G_E, G_T and G_R are the antenna gains of E, T and R, respectively.

Since the simple envelope detector is employed to perform the signal demodulation, once the amplitude difference between absorbing and reflecting states is too small to be discriminated, i.e., the ratio of signal strength for two states is lower than the demodulation sensitivity of receiver σ_R, the information would not be extracted successfully. In addition, when the signal strength of any states is lower than the work threshold of receiver δ_R, the envelope detector could not work properly and the communication would fail as well. Therefore, in order to eliminate the problem of phase cancellation in the link from T to R, the devices should be deployed in the proper locations where the following two conditions are satisfied:

$$\xi_{T\to R} = P_R^0 / P_R^1 \geq \sigma_R, \tag{8}$$

and

$$\zeta_{T\to R} = \min(P_R^1, P_R^0) \geq \delta_R. \tag{9}$$

B. Problem Formulation

Assume there are m stationary passive nodes denoted as $\mathcal{N} = \{n_1, n_2, \ldots, n_m\}$ distributed randomly in a 2D plane Ω. An exciter locates in the center of the plane providing carrier as well as energy for the nodes. Suppose we have k sinks and l relays, which are denoted as $\mathcal{S} = \{s_1, s_2, \ldots, s_k\}$ and $\mathcal{R} = \{r_1, r_2, \ldots, r_l\}$, respectively. Both sinks and relays can be deployed at any location in the area. The former is used to exchange information with sinks and relays, while the latter is employed to connect the deployed sinks. If no confusion is caused, we also use the notations to denote the locations of the corresponding devices. In this work, our aim is to use the minimal number of sinks and relays to form a connected network. To achieve this goal, we employ a two-step approach and formulate a Sink Deployment Problem (SDP) and a Relay Deployment Problem (RDP), which are defined as below.

Problem 1. Given a node set $\mathcal{N}$, SDP is to find a minimal sink set $\mathcal{S}' = \{s_1^*, s_2^*, s_3^*, \ldots\}$ that ensures each node in $\mathcal{N}$ is able to achieve reliable communication without phase cancellation, i.e.,

$$\textbf{(P1)} \quad \textit{minimize} \ |\mathcal{S}'|, \quad \textit{subject to} \ \mathcal{C}(s_1^*) \cup \mathcal{C}(s_2^*) \ldots \cup \mathcal{C}(s_{|\mathcal{S}'|}^*) = \mathcal{N}, \tag{10}$$

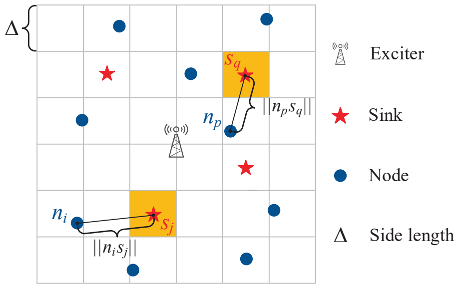

Fig. 2. Illustration of area discretization.

where $\mathcal{C}(s_x^*)$ is defined as the set of nodes that are able to communicate with sink s_x^* reliably.

Problem 2. Given a sink set $\mathcal{S}'$ which is determined by **P1**, RDP is to find a minimal relay set $\mathcal{R}'$ that is able to make all the deployed sinks connected, i.e.,

$$(\textbf{P2}) \quad \textit{minimize} \quad |\mathcal{R}'|, \qquad \textit{subject to} \quad \mathcal{S}' \textit{ is connected.} \tag{11}$$

III. Solution

In this section, we propose a greedy algorithm and a minimum-weight tree based algorithm to achieve the objective of eliminating phase cancellation and forming a reliable backscatter-based WPCN.

A. SDP Hardness Analysis

Theorem 1. The SDP is NP-complete.

Proof: We prove this by reducing the general NP-complete Set Cover Problem (SCP) [12] to SDP. The decision version of SCP can be defined as: given a universe $\mathcal{U} = \{u_1, u_2, \dots, u_p\}$ of p elements, an integer k, and a set $\mathcal{V} = \{\mathcal{V}_1, \mathcal{V}_2, \dots, \mathcal{V}_q\}$, which is a collection of subsets of $\mathcal{U}$, does there exist a sub-collection of $\mathcal{V}$ of size k that covers all elements of $\mathcal{U}$?

Based on this, we construct an instance of SDP: for each element $u_j \in \mathcal{U}$ and $\mathcal{V}_j \in \mathcal{V}$, we construct a node n_j and a sink s_j in SDP, respectively. For each element u_j in $\mathcal{V}_i$, we move n_j into the coverage of s_i if they are connected. Combining these together, we get the following special case of the decision version of the SDP: given a node set $\mathcal{N}$ of size p, a sink set $\mathcal{S}$ and an integer k, does there exist a subset of $\mathcal{S}$ of size k that covers all elements of $\mathcal{N}$? Thus, we can see that SDP is exactly SCP, which implies SDP is NP-complete. ■

B. Area Discretization

To address the challenge raised by the infinite solution space where the candidate locations of sinks and relays are continuous, we propose to discretize the 2D plane into multiple small subareas and specify a candidate point in each subarea to deploy the sink or relay. We emphasize that each point can be deployed with no more than one device.

As shown in Fig. 2, the continuous 2D plane Ω is evenly divided into $\Gamma = \lceil \frac{\Omega}{\Delta^2} \rceil$ uniform girds, where Δ is the side length of the grids. As the size of the grids is small enough, all the points in the same grid can be approximately considered as identical. Therefore, in our approach, the point locates in the center of the grid can be specified as the candidate point. Accordingly, once a grid is selected, the distance from node to each selected grid is approximated as the distance from the node to the center of the selected grid (refer to $\|n_i s_j\|$ and $\|n_p s_q\|$ in the Figure).

Algorithm 1: Greedy Algorithm for Sink Deployment

Input: Node set $\mathcal{N}$, number of sinks k, node sensitivity σ_n, sink sensitivity σ_s, node threshold σ_n, sink threshold σ_s and other necessary parameters.
Output: The selected sink set $\mathcal{S}'$.

Divide Ω into $\Gamma = \lceil \frac{\Omega}{\Delta^2} \rceil$ grids, and then get a finite set of candidate points $\mathcal{G}$.
Initial: $\mathcal{S}' = \emptyset$;
while $\mathcal{N} \neq null$ **do**
  for *each* $s_x \in \mathcal{G} \setminus \mathcal{S}'$ **do**
    for *each* $n_i \in \mathcal{N}$ **do**
      if $(\xi_{n_i \to s_x} \geq \sigma_s) \wedge (\zeta_{n_i \to s_x} \geq \delta_s)$ **then**
        if $(\xi_{s_x \to n_i} \geq \sigma_n) \wedge (\zeta_{s_x \to n_i} \geq \delta_n)$ **then**
          $\mathcal{C}(s_x) \leftarrow n_i$;
    for *each* $n_j \in \mathcal{N} \setminus \mathcal{C}(s_x)$ **do**
      for *each* $n_x \in \mathcal{C}(s_x)$ **do**
        if $(\xi_{n_j \to n_x} \geq \sigma_n) \wedge (\zeta_{n_j \to n_x} \geq \delta_n)$ **then**
          if $(\xi_{n_x \to n_j} \geq \sigma_n) \wedge (\zeta_{n_x \to n_j} \geq \delta_n)$ **then**
            $\mathcal{C}(s_x) \leftarrow n_j$;
  $s^* = \arg\max_{s_x \in \mathcal{G} \setminus \mathcal{S}'} (|\mathcal{C}(\mathcal{S}' \cup s_x)| - |\mathcal{C}(\mathcal{S}')|)$;
  if $|s^*| > 1$ **then**
    $s^* = \arg\max_{s_y \in s^*} (\sum_{i=0}^{m} (q_{n_i s_y} + \sum_{j=0}^{m} (q_{n_i n_j}))$;
  $\mathcal{N} = \mathcal{N} \setminus \mathcal{C}(s^*)$;
  $\mathcal{S}' = \mathcal{S}' \cup \{s^*\}$;
return $\mathcal{S}'$;

C. Solution to SDP

After area discretization, we get a set with finite candidate points, denoted as $\mathcal{G} = \{g_1, g_2, \dots, g_\Gamma\}$. Next, we propose a greedy algorithm (Algorithm 1) to solve the SDP. The first step of our algorithm is to traverse the whole candidate points to select the appropriate points where the nodes can communicate directly with the sink in both up and down links. Since nodes themselves can communicate with each other, i.e., they may also connect with one or even multiple nodes, except for the nodes directly connected to the sink, the nodes that indirectly connect with the sink should also be considered. However, due to the limited computation and storage capability, the communication among passive nodes is usually limited within one hop [13]. Thus, only the nodes that are two hops from the sink would be counted. Accordingly, our algorithm will iteratively select the point where the maximal passive nodes are covered once the sink is deployed. Here, the candidate sink location in each iteration would be:

$$s^* = \arg\max_{s_x \in \mathcal{G} \setminus \mathcal{S}'} (|\mathcal{C}(\mathcal{S}' \cup s_x)| - |\mathcal{C}(\mathcal{S}')|). \tag{12}$$

Nevertheless, in practice, there might exist multiple locations that cover the maximum number of nodes. To address

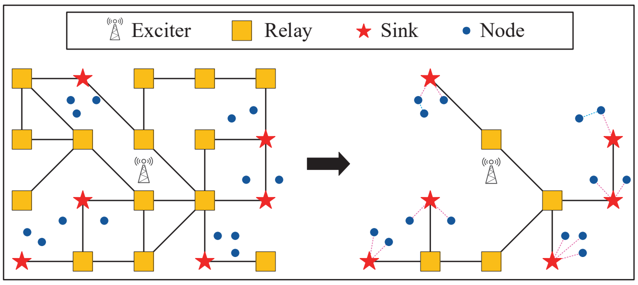

Fig. 3. The main process of our solution to RDP.

this issue, the concept of communication quality is introduced to further select the most suitable point. Note that the links in backscatter-based WPCN are non-symmetric, i.e., the performance of uplink (node to sink) and the downlink (sink to node) is different. Essentially, the performance of the link is determined by the received power. Specifically, on one hand, the bigger the power difference between absorbing and reflecting states, the better the link performs. On the other hand, a higher received power would also lead to a more stable link. Therefore, given u is communicating with v, the communication quality of link from u to v can be defined as:

$$q_{u\to v} = \begin{cases} 0, & \xi_{u\to v} < \sigma_v \ or\ \zeta_{u\to v} < \delta_v, \\ N(\xi_{u\to v}) + N(\zeta_{u\to v}), & other, \end{cases} \tag{13}$$

where $N(\cdot)$ represents the normalization operation, σ_v and δ_v are the demodulation sensitivity and work threshold of v, respectively. Based on this, we can further define the two-way communication quality q_{uv} as:

$$q_{uv} = \begin{cases} 0, & q_{u\to v} \cdot q_{v\to u} = 0, \\ (q_{u\to v} + q_{v\to u})/2, & other. \end{cases} \tag{14}$$

Thus, in each iteration, as long as there are more than one candidate points covering the maximum number of nodes at the same time, the point with the largest sum of communication quality will be selected:

$$s^* = \arg\max_{s_y \in s^*} \sum_{i=0}^{m} (q_{n_i s_y} + \sum_{j=0}^{m} (q_{n_i n_j})). \tag{15}$$

D. RDP Hardness Analysis

Theorem 2. The RDP is NP-hard.

Proof: We prove this by reducing the general NP-hard Steiner Tree Problem (STP) [12] to RDP. The decision version of STP can be defined as: given a bi-directed edge-weighted graph $\mathbb{A} = (\mathcal{V}, \mathcal{E})$, and a subset of nodes $\mathcal{V}' \in \mathcal{V}$, how to seek a minimum-weight tree that spans all nodes in $\mathcal{V}'$ using some of the nodes in $\mathcal{V} \setminus \mathcal{V}'$?

Let $\mathcal{S}'$ denote the set of deployed sinks, $\mathcal{G}_{\mathcal{R}}$ denote as the set of candidate locations of relays to be deployed, and $\mathcal{G}'_{\mathcal{R}}$ represent a subset of $\mathcal{G}_{\mathcal{R}}$. Based on this, we construct an instance of RDP: for the bi-directed edge-weighted graph, we construct $\mathbb{A}_r = (\mathcal{S}' \cup \mathcal{G}_{\mathcal{R}}, \mathcal{E})$, where the weight of $\mathcal{E}$ is the communication quality. Combining these together, we get the following special case of the decision version of the RDP: given a connected bi-directed graph $\mathbb{A}_r$ and a set of sinks $\mathcal{S}'$, does there exist a subset $\mathcal{G}'_{\mathcal{R}}$ that connects all the nodes in $\mathcal{S}'$ with minimum weight? Thus, we can see that RDP is exactly STP, which implies RDP is NP-hard. ■

Algorithm 2: Minimum-weight Tree Based Algorithm for Relay Deployment

Input: The obtained sink set $\mathcal{S}'$, the candidate relay location set $\mathcal{G}$ and other necessary parameters.
Output: The selected relay location set $\mathcal{R}'$.

Initial: $\mathcal{R}' = \emptyset$;
Construct a connection graph $\mathbb{G}$;
for *each* $uv \in E(\mathbb{G})$ **do**
  Assign edge weights to the edges in $\mathbb{G}$: $w(uv) = \frac{q_{max} - q_{uv}}{q_{max}} + 1$;
Apply the well-known Steiner Tree Algorithm to compute the minimum-weight Steiner tree $\mathbb{T}_r = (\mathcal{V}_{st}, \mathcal{E}_{st})$, which connects all sinks in $\mathcal{S}'$.
$\mathcal{R}' = \mathcal{V}_{st} \setminus \mathcal{S}'$.
return $\mathcal{R}'$.

E. Solution to RDP

To select the proper locations from the relay candidate locations, as shown in Fig. 3, we first construct a connection graph $\mathbb{G}$ for the network. The vertex set of $\mathbb{G}$ comprises of $\mathcal{S}'$ and the feasible candidate locations of relays $\mathcal{G} \setminus \mathcal{S}'$. The edge between vertices u and v exits when their two-way communication quality is not zero, i.e., $q_{uv} \neq 0$. Accordingly, as illustrated in Algorithm 2, we elaborate a weight function that is related to the communication quality and assign it to each edge $uv \in \mathbb{G}$:

$$w(uv) = \frac{q_{max} - q_{uv}}{q_{max}} + 1, \tag{16}$$

where $q_{max} \in [0, 1]$ is the maximum communication quality for all edge in $\mathbb{G}$. Then, let $\mathbb{H}$ be a subgraph of $\mathbb{G}$, the weight of $\mathbb{H}$ is thus expressed as:

$$w(\mathbb{H}) = \sum_{uv \in E(\mathbb{H})} w(uv) = 2|E(\mathbb{H})| - \sum_{uv \in E(\mathbb{H})} \frac{q_{uv}}{q_{max}}, \tag{17}$$

where $E(\mathbb{H})$ denotes the edge set of $\mathbb{H}$ and $|E(\mathbb{H})|$ denotes the length of $E(\mathbb{H})$. Utilizing such weight function, we can ensure that (1) the smaller the weight of the subgraph is, the fewer the edges as well as the vertices the subgraph would have; (2) when comparing two subgraphs with the same edge number, the one who has the smaller weight would perform better as it has a higher communication quality.

Thus, we can transform the problem of minimizing the number of relays into the problem of finding a minimum-weight tree that spans all the deployed sinks and our problem **(P2)** can be reformulated as an STP:

$$\begin{aligned} \textbf{(P2')} \quad & minimize \quad w(\mathbb{H}), \\ & subject\ to \quad \mathbb{H} \subseteq \mathbb{G}\ and\ \forall v \in \mathcal{S}', v \in \mathbb{H}. \end{aligned} \tag{18}$$

Hence, we can address **P2'** with the well-known Steiner Tree algorithm [14]. The output $\mathbb{T}_r = (\mathcal{V}_{st}, \mathcal{E}_{st})$ is a minimum-weight tree with all sinks being connected to relays, where

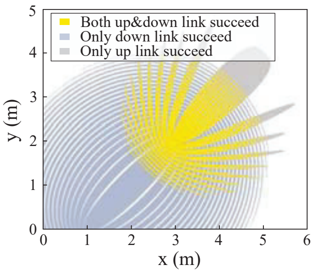

Fig. 4. A distribution example of phase cancellation

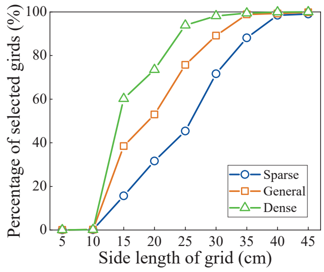

Fig. 5. Δ versus percentage of selected grids

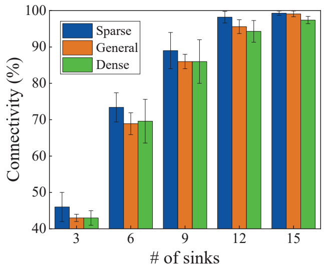

Fig. 6. Number of sinks versus connectivity

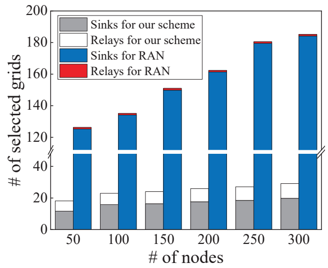

Fig. 7. Number of nodes versus number of selected grids

$\mathcal{V}_{st}$ and $\mathcal{E}_{st}$ represent the vertex and edge set of $\mathbb{T}_r$. By removing the vertices indicating the sink locations from the tree, i.e., $\mathcal{V}_{st} \setminus \mathcal{S}'$, we can finally get the location set that the number of relays is minimized and the communication quality is guaranteed in the meanwhile.

IV. SIMULATIONS

In this section, we evaluate the performance of the proposed deployment scheme through extensive experiments under different network settings.

A. Simulation Setup

In the simulations, we employ the communication model presented in Section II-A. For the exciter, we set the output power as 36dBm and its antenna gain G_E as 8.5dBi. The wavelength of the excitation signal is set as $0.33m$. For the backscatter-based passive nodes, we set the antenna gain G_n as 2dBi and its reflecting coefficient γ_n as 0.8. The demodulation sensitivity σ_n as 0.1 and the work threshold δ_n as -6.3dB. Without loss of generality, we set the phase change introduced by reflection as $\phi = 0$ for computation simplicity.

Considering that sinks not only need to collect information from the nodes but forward data to the nodes, the sinks should be equipped with a better communication capability than the passive nodes. We set sinks' antenna gain G_s, reflecting coefficient γ_s, demodulation sensitivity σ_s and the work threshold δ_s as 4.8dBi, 0.9, 0.08 and -9.3dB, respectively. Moreover, considering that the relays are responsible for processing the data of the whole network, they should be equipped with the best communication capability. Thus, to evaluate the performance of our proposed algorithms, we correspondingly set the parameters for relays as G_r = 6dBi, γ_r = 0.95, $\sigma_r = 0.1$ and $\delta_r = -10$dB.

B. Performance

To validate our proposed model, we first consider a simple communication scenario with an exciter, a backscatter-based passive node and a sink. The exciter and node are fixed at coordinates (1, 0) and (3, 2), respectively, and the sink can be placed at any location in the $6m \times 5m$ plane. We emphasise that phase cancellation might happen between any two backscatter-based devices, adding more devices will not provide more insights for our problem and solution. As shown in Fig. 4, phase cancellation has a severe effect on the connectivity of the backscatter-based WPCN. Specifically, the node and the sink could exchange information in both directions only when the sink locates in the yellow area. However, when the sink is placed in the blue or grey area, the phase cancellation would lead to a communication failure, i.e., either in the uplink or in the downlink. Even worse, when the sink locates in the blank area, the communication can not succeed in both uplink and downlink. Therefore, with the proposed model as a guidance, the phase cancellation problem can be fundamentally eliminated by elaborating the deployment of sinks and relays.

Then, we evaluate how the side length of grid Δ impacts the number of sinks required in our proposed greedy algorithm for sink deployment under sparse, general and dense scenarios, where the node density are 0.5, 1 and 2 nodes$/m^2$, respectively. As shown in Fig. 5, the percentage of selected grid (i.e., the ratio of the selected grids to the total number of candidate grids) increases significantly when Δ exceeds $10cm$, this is because the total number of candidate points will decrease dramatically with the increasing of Δ, and the number of candidate points that is able to cover multiple nodes will decrease accordingly. Thus, our algorithm needs to select more grids to cover all the nodes in the field. However, we also observed that the percentage of selected grid increases slightly when Δ increases from $5cm$ to $10cm$ under these three scenarios. Therefore, to save the running time without significant decreasing the performance of the our algorithm, we can set Δ as $10cm$.

Moreover, to further evaluate the performance of our proposed greedy algorithm, we also investigate how the sink deployment impacts the connectivity of the network. Similarly, the simulation are conducted under the three aforementioned scenarios. The connectivity is defined as the proportion of nodes that are covered by sinks, and size of the plane is $100m^2$. Fig. 6 shows that our algorithm can achieve a considerable connectivity through deploying a very small amount of sinks. Specifically, with only 6 sinks, on average 73.4%, 68.9% and 69.6% of passive nodes are covered under sparse, general and dense scenarios, respectively. Furthermore, once the number of sinks increased to 12, the corresponding connectivity would accordingly increased to 98.2%, 95.6% and 94.3%.

To the best of our knowledge, we are the first deployment scheme that aims to eliminate the phase cancellation in backscatter-based WPCN. Therefore, we introduce a RANdom sink deployment (RAN) algorithm which randomly selects a

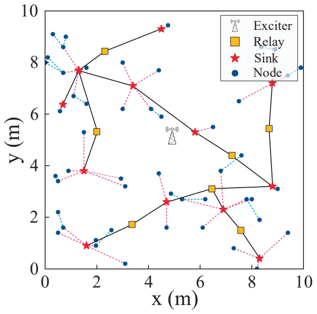

Fig. 8. Visualization of a instance with 50 nodes

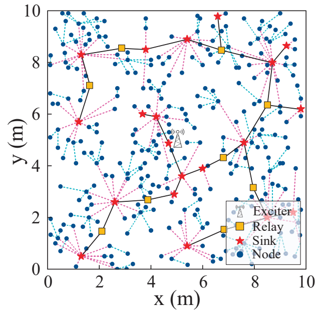

Fig. 9. Visualization of a instance with 300 nodes

grid from the candidates to deploy the sink and repeats until all nodes are connected for comparison. Simulation results in Fig. 7 show that when the number of nodes varies from 50 to 300, the number grids required for sinks and relays increase from 18.2 (11.7 for sink and 6.5 for relay) to 29.1 (19.8 for sink and 9.3 for relay) on average. However, RAN eventually requires around 125.3 and 184.2 grids when the number of nodes are 50 and 300, respectively. For easy understanding, we also visualize the deployments of sinks and relays for 50 nodes and 300 nodes in Fig. 8 and Fig. 9, respectively. We can see from the figures that, after deploying a small number of sinks and relays, the connectivity and reliability of the network can be guaranteed.

V. Related Work

In the literature, how to elaborate the deployment of the network to ensure reliability and connectivity has been widely studied. For example, Boubrima et al. proposed a minimum-cost deployment scheme which not only sustains the connectivity but guarantees the coverage [15]. Hajjej et al. presented a deployment approach that approximates the optimal trade-off among coverage, lifetime and energy dissipation while maintaining connectivity of the network [16]. By introducing high-altitude platforms as relays, Zhu et al. designed an effective deployment algorithm to minimize the power consumption of the space-air-ground network [17]. However, these aforementioned schemes are not applicable as phase cancellation only occurs in the backscatter-based WPCNs.

To alleviate the severe impact incurred by phase cancellation, a widely used way is to transmit the same information by selecting different load impedances. For instance, Shen et al. proposed a multi-phase backscatter technique to reduce the phase cancellation problem by sending every packet twice with a phase offset [9]. Similarly, Qian et al. employed a high-order phase modulation scheme that achieves a considerable data rate [18]. However, these approaches would lead to a significant decrease in the transmission throughput. Besides, employing additional antennas is another way to provide signal diversity. Braidio combated phase cancellation by employing two receiving antennas and picking only these with perceptible amplitude difference [19]. AnyScatter utilized all nearby single-stream wireless devices for backscatter transmission and addressed phase cancellation by designing a parallelized backscatter receiver with multiple antennas [20]. Nevertheless, these solutions will increase the cost as well as the size of the nodes. Additionally, Ryoo et al. realized a practical backscatter-based WPCN and leveraged multihop to reduce the transmission failure caused by phase cancellation [10]. Majid et al. further proposed a protocol suite to extend the coverage of the multihop backscatter-based WPCN [11]. However, the reliability is still not guaranteed as the phase cancellation problem is not fundamentally eliminated.

VI. Conclusions

In backscatter-based WPCNs, the connectivity and reliability of the network are severely affected by phase cancellation. In this work, we investigate the phase cancellation problem by revealing the relationship between locations of communication participants and communication quality. To this end, a two-stage solution is presented. Firstly, a greedy algorithm is first proposed to deploy minimum number of sinks to connect all nodes in the field. Then, a minimum-weight tree based algorithm is introduced to connect the deployed sinks with the minimum number of relays. Extensive simulations are conducted to show our superior performance.

References

[1] J. Zhao *et al.*, "X-Tandem: Towards Multi-Hop Backscatter Communication with Commodity WiFi," in *ACM MobiCom*, 2018, pp. 497–511.
[2] S. Zhou *et al.*, "Ergodic rate analysis of cooperative ambient backscatter communication," in *IEEE WCL*, 2019, pp. 1679–1682.
[3] P. Zhang *et al.*, "Enabling practical backscatter communication for on-body sensors," in *ACM SIGCOMM*, 2016, pp. 370–383.
[4] A. Wang *et al.*, "FM backscatter: Enabling connected cities and smart fabrics," in *USENIX NSDI*, 2017, pp. 243–258.
[5] V. Liu *et al.*, "Ambient backscatter: Wireless communication out of thin air," in *ACM SIGCOMM*, 2013, pp. 39–50.
[6] D. Niyato *et al.*, "Wireless powered communication networks: Research directions and technological approaches," in *IEEE Wireless Communications*, 2017, pp. 88–97.
[7] J. Ryoo *et al.*, "Barnet: Towards activity recognition using passive backscattering tag-to-tag network," in *ACM MobiSys*, 2018, pp. 414–427.
[8] A. Ahmad *et al.*, "Enabling passive backscatter tag localization without active receivers," in *ACM SenSys*, 2021, pp. 178–191.
[9] Z. Shen *et al.*, "Phase cancellation in backscatter-based tag-to-tag communication systems," in *IEEE IoTJ*, 2016, pp. 959–970.
[10] J. Ryoo *et al.*, "Design and evaluation of "BTTN": A backscattering tag-to-tag network," in *IEEE IoTJ*, 2018, pp. 2844–2855.
[11] A. Y. Majid *et al.*, "Multi-hop backscatter tag-to-tag networks," in *IEEE INFOCOM*, 2019, pp. 721–729.
[12] V. V. Vazirani, *Approximation algorithms*. Springer, 2001.
[13] J. Zhao *et al.*, "Towards scalable backscatter sensor mesh with decodable relay and distributed excitation," in *ACM MobiSys*, 2020, pp. 67–79.
[14] L. Kou *et al.*, "A fast algorithm for steiner trees," in *Acta informatica*, 1981, pp. 141–145.
[15] A. Boubrima *et al.*, "Optimal WSN deployment models for air pollution monitoring," *IEEE TWC*, pp. 2723–2735, 2017.
[16] F. Hajjej *et al.*, "A new optimal deployment model of internet of things based on wireless sensor networks," in *IEEE IWCMC*, 2019, pp. 2092–2097.
[17] C. Zhu *et al.*, "Optimal HAP deployment and power control for space-air-ground iort networks," in *2021 IEEE WCNC*, 2021, pp. 1–7.
[18] J. Qian *et al.*, "IoT communications with M-PSK modulated ambient backscatter: Algorithm, analysis, and implementation," in *IEEE IoTJ*, 2019, pp. 844–855.
[19] P. Hu *et al.*, "Braidio: An integrated active-passive radio for mobile devices with asymmetric energy budgets," in *ACM SIGCOMM*, 2016, pp. 384–397.
[20] T. Kim and W. Lee , "Anyscatter: Eliminating technology dependency in ambient backscatter systems," in *IEEE INFOCOM*, 2020, pp. 287–296.